Northward ITCZ shift drives reduced ENSO activity in the Mid-Pliocene Warm Period

Gabriel Pontes (gabrielpontes@usp.br)
University of São Paulo https://orcid.org/0000-0003-4397-4238

Andrea Taschetto
UNSW https://orcid.org/0000-0001-6020-1603

Alex Sen Gupta
The University of New South Wales https://orcid.org/0000-0001-5226-871X

Agus Santoso
The University of New South Wales https://orcid.org/0000-0001-7749-8124

Ilana Wainer
Instituto Oceanogr&#x00E1 https://orcid.org/0000-0003-3784-623X

Alan Haywood
University of Leeds

Wing-Le Chan
The University of Tokyo https://orcid.org/0000-0002-5646-6104

Ayako Abe-Ouchi
University of Tokyo https://orcid.org/0000-0003-1745-5952

Christian Stepanek
Alfred Wegener Institute Helmholtz Centre for Polar and Marine Research https://orcid.org/0000-0002-3912-6271

Gerrit Lohmann
Alfred Wegener Institute https://orcid.org/0000-0003-2089-733X

Stephen Hunter
University of Leeds https://orcid.org/0000-0002-4593-6238

Julia Tindall
University of Leeds https://orcid.org/0000-0002-2360-5761

Mark Chandler
Columbia University-NASA/GISS

Linda Sohl
Columbia University

Dick Peltier
University of Toronto

Deepak Chandan
University of Toronto

Youichi Kamae
University of Tsukuba
Kerim Nisancioglu
University of Bergen
Zhongshi Zhang
China University of Geosciences https://orcid.org/0000-0002-2354-1622
Camille Contoux
Laboratoire des Sciences du Climat et de l'Environnement, LSCE/IPSL
Ning Tan
Key Laboratory of Cenozoic Geology and Environment, Institute of Geology and Geophysics, Chinese Academy of Sciences,
Qiong Zhang
Stockholm University https://orcid.org/0000-0002-9137-2883
Bette Otto-Bliesner
National Center for Atmospheric Research https://orcid.org/0000-0003-1911-1598
Esther Brady
National Center for Atmospheric Research
Ran Feng
University of Connecticut
Anna von der Heydt
Utrecht University
Michiel Baatsen
University of Utrecht https://orcid.org/0000-0002-0123-7005
Arthur Oldemann
Utrecht University

Article

Keywords: El Niño Southern Oscillation (ENSO), ocean science, Mid-Pliocene Warm Period

Posted Date: June 22nd, 2021

DOI: https://doi.org/10.21203/rs.3.rs-402220/v1

Version of Record: A version of this preprint was published at Nature Geoscience on August 11th, 2022. See the published version at https://doi.org/10.1038/s41561-022-00999-y.

Northward ITCZ shift drives reduced ENSO activity in the Mid-Pliocene Warm Period

Gabriel M. Pontes[*1], Andréa S. Taschetto[2,3], Alex Sen Gupta[2,3], Agus Santoso[2,3,4], Ilana Wainer[1], Alan Haywood[5], Wing-Le Chan[6], Ayako Abe-Ouchi[6], Christian Stepanek[7], Gerrit Lohman[7], Stephen Hunter[5], Julia C. Tindall[5], Mark A. Chandler[8], Linda E. Sohl[8], W. Richard Peltier[9], Deepak Chandan[9], Youichi Kamae[10], Kerim H. Nisancioglu[11], Zhongshi Zhang[11], Camille Contoux[12], Ning Tan[12,13], Qiong Zhang[14], Bette Otto-Bliesner[15], Esther C. Brady[15], Ran Feng[16], Anna S. von der Heydt[17], Michiel L. J. Baatsen[17], Arthur M. Oldeman[17]

*Corresponding author: Gabriel M. Pontes (gabrielpontes@usp.br)

[1]Oceanographic Institute, University of São Paulo, São Paulo, Brazil
[2]Climate Change Research Centre, The University of New South Wales, Australia
[3]ARC Centre of Excellence for Climate Extremes, The University of New South Wales, Australia
[4]Centre for Southern Hemisphere Oceans Research, CSIRO Oceans and Atmosphere, Hobart, Tasmania, Australia
[5]School of Earth and Environment, University of Leeds, Leeds, UK
[6]Centre for Earth System Dynamics, Atmosphere and Ocean Research Institute, University of Tokyo, Japan
[7]Alfred Wegener Institute, Helmholtz Centre for Polar and Marine Research, Bremerhaven, Germany
[8]NASA/GISS, Columbia CCSR, Columbia University, New York, NY 10025, USA
[9]Department of Physics, University of Toronto, Toronto, Canada
[10]Faculty of Life and Environmental Sciences, University of Tsukuba, Tsukuba, Japan
[11]NORCE Norwegian Research Centre, Bjerknes Centre for Climate Research, 5007 Bergen, Norway
[12]Laboratoire des Sciences du Climat et de l'Environnement, LSCE/IPSL, CEA-CNRS-UVSQ Université Paris-Saclay, 91191 Gif-sur-Yvette, France
[13]Key Laboratory of Cenozoic Geology and Environment, Institute of Geology and Geophysics, Chinese Academy of Sciences, Beijing 100029, China
[14]Department of Physical Geography and Bolin Centre for Climate Research, Stockholm University, Stockholm, 10691, Sweden
[15]National Center for Atmospheric Research, Boulder, USA
[16]Department of Geosciences, College of Liberal Arts and Sciences, University of Connecticut, Storrs, CT 06033, USA
[17]Institute for Marine and Atmospheric research Utrecht (IMAU), Department of Physics, Utrecht University, Utrecht, 3584 CS, the Netherlands

The El Niño Southern Oscillation (ENSO) is the strongest pattern of year-to-year climate variability found in the equatorial Pacific Ocean with global impacts. However, it is not fully understood how ENSO responds to different warming scenarios. In the warmer climate (~2-3K) of the mid-Pliocene Warm Period (~3 Ma BP), models consistently suggest a weakening of ENSO variability, with a mean reduction of 25% (±16%). We show that a near unanimous weakening of ENSO across models cannot be fully explained simply by mean state changes in the equatorial Pacific Ocean. Instead, robust off-equatorial mean state changes in the mid-Pliocene are not favourable for ENSO activity. A northward displacement of the Pacific Inter-Tropical Convergence Zone (ITCZ) is found to be significantly linked to the ENSO weakening across models. This is accompanied by increased south-easterly trade winds in the western Pacific and an intensified South Pacific Subtropical High, which are consistent with suppressed activity of processes that initiate ENSO. Our results provide a constraint to past and future changes to ENSO associated with the climatological ITCZ position.

ENSO warm (El Niño) and cold (La Niña) events cause significant changes in weather patterns and ocean circulations, impacting on agriculture, fisheries, coral bleaching, cyclogenesis, among a host of other impacts[1]. Given its pronounced social and economic impacts and potential predictability of a few seasons in advance, ENSO has been a subject of intense investigation[2]. Whether and how ENSO changes in response to greenhouse and other external forcings may be studied by investigating past, present, and future climates with paleo-reconstructions, instrumental records, and numerical simulations. There is a

lack of consensus among climate models as to how ENSO characteristics, such as amplitude and flavour, will respond to future warming[3–7]. Nonetheless, recent studies show that models that are better at capturing ENSO nonlinearity tend to simulate enhanced sea surface temperature (SST) variability in the eastern equatorial Pacific[8] and increased frequency of events that exhibit intensified ENSO characteristics[9,10]. The increased frequency is attributed to changes in the Pacific mean state which is marked by a weakened Walker Circulation, increased upper-ocean stratification, and equatorially enhanced warming that causes the Intertropical Convergence Zone (ITCZ) to be displaced equatorward[10–12].

Studies based on paleo-reconstructions have also indicated that ENSO activity is sensitive to the mean climate. A synthesis of mid-Holocene (~6 ka [thousand years] BP) records indicates a 33% reduction in ENSO amplitude in the eastern Pacific during this period[13]. ENSO activity over the last millennium was shown to be weaker when compared to the last half-century[14], potentially suggesting global warming induced changes. Furthermore, there is evidence of significantly reduced ENSO variability during the last interglacial period[15] (~127 ka BP). However, proxy data for the Pliocene (~5 to ~3 Ma [million years] BP) are controversial on tropical Pacific changes[16–18]. A Pliocene El-Niño like mean state has been hypothesized to reduce ENSO variability[18], although there is evidence of significant interannual variability during this period[19]. As such, tropical Pacific mean state changes during the mid-Pliocene and how it has impacted ENSO activity are still uncertain.

If there was a time in the distant past that provides an analogue to a warmer end-of-century climate, it would be the mid-Pliocene Warm period (mPWP; ~3.3Ma BP)[20].

The mPWP was marked by warmer SSTs of up to 9 K and 4 K in the Northern and Southern Hemisphere, respectively[21], compared to pre-industrial times (~1850 Common Era), with orbital forcing[22] and elevated atmospheric CO_2 concentrations similar to present day[23] (~400 ppm) while polar ice was reduced[24]. Partly motivated by the similarities between the mPWP and scenarios of future projected warming, the Pliocene Model Intercomparison Project (PlioMIP)[25,26] initiative was developed. Here we examine the broad PlioMIP ensemble, including phases 1 and 2, to better understand how ENSO activity might change under warmer climates.

Reduced ENSO amplitude

The PlioMIP ensemble simulate a significant reduction in the amplitude of SST variability across most of the global tropics (Figure 1a; see Supplementary Figure S1 for PlioMIP1). In the Indian Ocean, there is a robust weakening in the western sector while no significant changes in the eastern sector (Figure 1a). The tropical Atlantic shows reduced SST variability in both sides of the equator likely indicating reduced variability of the Atlantic Meridional Mode[27] (Figure 1a). The most pronounced weakening of tropical variability occurs in the equatorial Pacific (Figure 1a). The reduced amplitude in SST variability in the eastern equatorial Pacific (Niño 3 region; 5ºN-5ºS; 150º-90ºW) is simulated by 21 out of 23 PlioMIP models (including phases 1 and 2 of PlioMIP). Considering PlioMIP2 models only, there is a multi-model mean amplitude reduction of 25% (±16% standard deviation; Figure 1b).

Separating the Niño3 variability change into interannual and longer timescales (>10 yrs) components shows that all but one model simulate reduced amplitude in the

interannual band (Supplementary Figure S2), a timescale that is dominated by ENSO. Additionally, 75% (17 out of 23) of the models indicate a tendency for a shift towards lower frequencies as indicated by either an increased amplitude at low-frequency (>10 yr) or a more pronounced weakening at interannual than on longer time scales (Supplementary Figure S2). However, changes in decadal or longer periods must be further evaluated using longer timeseries data. Here due to data availability, we only use the last 100 years of each model's simulation.

Role of Equatorial Pacific Ocean changes

ENSO dynamics is mostly dominated by equatorial processes, which are influenced by the background state[28]. The PlioMIP models simulate a basin-wide surface warming of the Equatorial Pacific (Figure 2a). The multi-model mean indicates higher levels of warming in the eastern Pacific, although there are large inter-model differences in this pattern[29] (Supplementary Figures S3 and S4). These are likely associated with differences in wind changes, suggestive of wind-evaporation-SST feedback, especially in the eastern Pacific[30] (Figure 2a, see Supplementary Figure S5 for PlioMIP1). Of particular importance for ENSO dynamics are changes in equatorial thermal gradients. Recent studies have shown the importance of changes in the oceanic zonal equatorial dynamics[9,31] and vertical equatorial gradients[8] to our understand on how ENSO might change in the future.

Firstly, we evaluate changes in the thermocline slope as a proxy for changes in equatorial ocean dynamics. Strong (weak) westward equatorial currents drive increased (decreased) east-west thermocline slope, as it shoals (deepens) the eastern thermocline while deepening (shoaling) its western sector[9]. We find that models with a steeper mean

131 thermocline in the mPWP (i.e. a La Niña-like mean state) are typically associated with
132 larger ENSO amplitude reductions, while a flatter mean thermocline (i.e. an El Niño-like
133 state) is associated with either an slight increase or a weak decrease in ENSO variability
134 (r=-0.52; Figure 2b). This indicates that equatorial Pacific mean state with a steeper
135 thermocline, which corresponds to intensified ocean-atmosphere circulations, is less
136 favourable to strong ENSO variability. Under such La Niña-like mean state, stronger initial
137 anomalies are required to substantially weaken the climatological states in order to provide
138 favourable conditions for strong El Niño development[9].

139 We further examine possible changes in the equatorial oceanic conditions that could
140 be unfavourable to ENSO development[18,32]. Ocean stratification has been hypothesized to
141 influence the variability of extreme ENSO events, as an increased ocean stratification
142 would tend to increase the dynamical coupling between the ocean and the atmosphere[8]. As
143 such, we evaluate ocean stratification in the central-west Pacific near the warm pool edge,
144 a region of maximum wind variability and where wind anomalies trigger ocean waves and
145 initiate ENSO development. Indeed, we find that models with decreased ocean
146 stratification are associated with major ENSO reductions, and the reduction is weaker with
147 increased ocean stratification (Figure 2c). However, an increased stratification seen in nine
148 models cannot support the fact that the ENSO variability is reduced in each of seven of
149 those models. A similar inconsistency also applies for the thermocline slope change
150 (Figure 2b). Thus, while changes in the thermocline and stratification help to explain inter-
151 model differences in ENSO amplitude changes, there must be other processes that apply
152 across models, which provide an explanation for the overall weakening of ENSO
153 variability.

Off-Equatorial Pacific changes

Whilst ENSO development is closely related to the zonal equatorial dynamics[28], ENSO events are also affected by a variety of other large-scale processes beyond the equatorial Pacific[10,33,34]. For instance, changes to the mean meridional SST gradient or processes in the extratropics can play an important role in triggering ENSO events. In particular, all PlioMIP models simulate a weaker equator-to-pole temperature gradient associated with polar amplified warming[35].

To investigate processes outside the equatorial Pacific, we first evaluate the role of meridional SST gradients through possible displacements of the ITCZ in the mPWP. Southward (northward) ITCZ displacements, due to changes in off-equatorial SST gradients, have been shown to affect ENSO activity through increased (reduced) probability of occurrences of deep convection in the central-eastern Pacific[11]. Here we show that a mean northward ITCZ shift during austral spring-summer, i.e., during developing and mature ENSO phases, is significantly related to the ENSO weakening across models (Figure 3a). This northward shift in the ITCZ generally acts to supress El Niño development, via a reduced probability of deep convection occurrences in the eastern Pacific[11]. To illustrate this, we evaluate models' performance in simulating the non-linear relationship between ENSO SST anomalies and anomalous precipitation events in the eastern Pacific (see Methods; Supplementary Figure S6). Five models correctly simulate this characteristic and indicate that the further north the mean ITCZ migrates the less probable are occurrences of anomalous rainfall events in the eastern Pacific associated with

ENSO SST anomalies (Figure 3b-f). The ITCZ shift can fully explain ENSO weakening across these 5 models (r=0.99; Supplementary Figure S7).

We also evaluate possible changes to the processes that are known to initiate ENSO events. Firstly, the reversal of the circulation of easterly trade winds in the western Pacific is known to initiate ENSO development[36]. In the PlioMIP models, the annual mean intensification of the western Pacific trade winds corresponds with weaker wind variability over this region (Figure 4a). Climatologically stronger easterly trades tend to inhibit: 1) the stochastic forcing of westerly wind bursts in the western Pacific[37] that triggers the positive thermocline feedback; 2) southward shifts of the ITCZ through positive Wind-Evaporation-SST feedback which cools the equatorial Pacific Ocean, thereby increasing the meridional SST gradient; and 3) eastward displacements of the Walker circulation.

Secondly, we evaluate the South Pacific Meridional Mode (SPMM), which induces an anomalous zonal pressure dipole across the tropical South Pacific that facilitates westerly wind anomalies in the equatorial region, acting as a precursor for strong El Niño events[34]. We find that all but two PlioMIP2 models simulate a decreased amplitude of the SPMM in the mPWP (Figure 4b). Finally, extreme El Niño events have been shown to be amplified by an anomalous zonal pressure dipole in the Southern Hemisphere[33]. In such condition, an anomalous high pressure over Australia facilitates cold surges through the Coral Sea, called the Southern Hemisphere Booster (SHB)[33], that promote westerly wind anomalies in the western Pacific conducive for El Niño development. The meridional wind variability in the SHB region also decreases in 10 out of 12 PlioMIP2 models in the mPWP simulations (Figure 4c). These aforementioned changes are associated with reduced

probability of El-Niño initiation that would otherwise contribute to stronger ENSO variability.

Large-scale forcing

The Pacific ITCZ-ENSO relationship demonstrated in the previous section can be either a result of a large-scale global ITCZ shift modulating ENSO or a local response of the Pacific ITCZ to changes in ENSO activity. The PlioMIP models indicate that the northward shift of the ITCZ during the mPWP occurs in all basins, given the typical rainfall fingerprint of a meridional dipole change found across the global tropics (Figure 5a; see Supplementary Figure S8 for PlioMIP1). Additionally, the PlioMIP models systematically simulate polar amplified warming in both hemispheres (Figure 5b), which can give rise to large-scale changes in the meridional temperature gradient and affect the ITCZ position through changes in atmospheric heat fluxes[39].

To further evaluate the cause of the ITCZ shift, we performed sensitivity experiments using the NCAR Community Atmospheric Model version 4 (CAM4; See Methods). The atmospheric model experiments forced with PlioMIP mean SSTs allow us to isolate changes in atmospheric features and circulation, due to mPWP surface warming, from changes in climate variability such as ENSO. It is worth noting the mPWP climatological-mean warming pattern, used to force the atmospheric model, may still contain some non-linear influence of ENSO changes, but here we assume these are negligible (see Methods). We also investigate the link between the global ITCZ shift to possible changes in the large-scale inter-hemispheric temperature contrast through energetic constraints.

In the present climate, during austral summer, the ITCZ shifts southwards toward the equator due to increased insolation in the Southern Hemisphere of which the excess heat is transported to the Northern Hemisphere (implying a northward energy flux across the equator), through an intensification of the Northern Hemisphere Hadley circulation[40]. In the mid Pliocene, the CAM4 model simulates a decreased northward heat transport across the equator during the austral summer (Figure 5c). Due to the mutual relationship between changes in the energy flux across the equator and ITCZ position, a decreased northward energy flux at the equator is accompanied by a northward ITCZ shift. This result from a reorientation of the meridional circulation of the atmosphere within the tropics. Higher rates of warming in the Northern Hemisphere drive an intensification and northward expansion of the Southern Hemisphere Hadley cell and weaker circulation in the Northern counterpart (Figure 5d; see Supplementary Figure S8 for PlioMIP1), which reduces the atmospheric energy input from the Southern to the Northern Hemisphere during the austral summer.

The CAM4 experiments suggest that the meridional displacement of the ITCZ is a global feature of the PlioMIP simulations and occurs due to the mean mPWP warming. One of the most robust features of the mPWP simulations is the polar amplified warming, especially in the Northern Hemisphere which increases the inter-hemispheric temperature gradient (Figure 5b). However, whether the mPWP ITCZ shift is a response to tropical or extratropical warming is still an open question. For instance, CAM4 experiments indicate an overall decrease in the northward atmospheric heat transport (AHT) in the Northern Hemisphere and overall increase in the southward AHT in the Southern Hemisphere (Figure 5b), which initially points to changes in pole-to-pole temperature gradient.

The large-scale changes in the meridional circulation likely induce changes in horizontal circulation. Meridional displacements of the ITCZ have been shown to affect trade winds in the Atlantic basin[41]. In the Pacific Ocean, the PlioMIP models indicate that a northward ITCZ shift is significantly related to intensified western Pacific trades (Figure 5d), which is analogous to synchronized shifts of the Walker and Hadley circulations during different ENSO phases[42]. An analysis of the global low-level circulation indicates that the anomalously stronger western trades in the mPWP are sourced at the subtropical South Pacific due to an intensified circulation of the South Pacific Subtropical High system (Figure 5e; see Supplementary Figure S8 for PlioMIP1). These changes are not exclusive to the South Pacific but occur in all ocean basins (Figure 5e). The synchronized changes in the meridional and zonal atmospheric circulation are likely a result of global changes in atmospheric heat fluxes during the warmer mPWP. Thus, this illustrates a possible influence of changes in global atmospheric dynamics on ENSO in a warmer climate.

Discussion

The results presented here suggest a link between reduced ENSO amplitude and the northward shift of the ITCZ in the mPWP, associated with stronger climatological circulation in the Southern Hemisphere (Figure 6). The northward shift of the ITCZ reduces the probability of occurrence of ENSO-related rainfall events in the eastern Pacific (Figure 6). Enhanced mean western Pacific trade winds are associated with reduction in the variability and, thus, possibly the occurrences of stochastic westerly wind anomalies (Figure 6). A strengthened Southern Hemisphere Subtropical High pressure system in the Pacific, and intensified Southern Hemisphere Hadley circulation are thought to be a

response to enhanced Northern Hemisphere warming through changes in the inter-hemispheric meridional heat fluxes[43] via energetic constraints for the ITCZ position[39,44]. An intensified South Pacific Subtropical High weakens and shifts the South Pacific Convergence Zone polewards[43], reducing its interaction with equatorial processes, and may suppress zonal sea-level pressure anomalies imposed by the South Pacific Meridional Mode and the Southern Hemisphere Booster, which otherwise favour ENSO development (Figure 6). As such, the climatological stability imposed by intensified tropical Southern Hemisphere circulation acts to increase ENSO stability, as ENSO by definition is a deviation from the mean climate, and thus stronger climatological circulations can be viewed as unfavourable to ENSO-induced changes[10].

In addition to the reduced ENSO amplitude, SST variability in other tropical basins is also found to decrease (Figure 1a). This may contribute to weakened ENSO variability via pan-tropical interactions[45] due to a delayed and weaker negative feedback[46,47], although reduced variability in other tropical basins itself might also be a consequence of reduced ENSO variability. For instance, an anomalously warm tropical North Atlantic is known to support the initiation of La Niña events[48]. Pontes et al.[27] reported that all PlioMIP1 models simulate reduced tropical North Atlantic variability associated with a warming of this basin and northward Atlantic ITCZ shift. Taken together, these results suggest that a northward shift of the global ITCZ can likely mute tropical Pacific and Atlantic SST variability.

Our results are subject to a number of uncertainties in the simulations tied to sparse and limited proxy data, which are used to constrain the PlioMIP experiments, and systematic climate model biases[49]. Changes in the inter-hemispheric SST gradient for example could be affected by uncertainties in the extension of the mPWP ice sheets[50,51],

poor representation of certain polar feedbacks[52] (i.e. interactive land-ice), climate sensitivity[53], and biases in tropical convection and SST of the climate models, such as double-ITCZs[54] and an overly strong cold tongue. Despite data uncertainties and different model biases, we show that the current generation of climate models simulate a robust response of ENSO to changes in the ITCZ position in a warmer past climate.

With respect to future warming, paleoclimate studies have been investigating whether there was a past warm climate that would serve as an analogue to the current warming. Our findings indicate that, although the mPWP surface warming is comparable in magnitude as projected toward the end of 21st century under a 'business as usual' scenario (~3K)[20], ENSO shows an opposite response to that projected[8,11]. It is worth noting the mPWP exemplifies an equilibrium climate with similar CO_2 concentration as today, indicating we could end-up in a similar-to-Pliocene climate if CO_2 is maintained at present levels once a steady state is reached. However, the current rate of atmospheric CO_2 rise is unprecedented in Earth's history, which differs from how Earth has warmed in the past. Thus, linking past and future warmings is not straightforward. Here the evaluation of the mPWP shows that in an empirically based equilibrium warming a northward ITCZ shift drives reduced ENSO activity. If this mechanism can be applied to the 21st century projections where a southward shift of the Pacific ITCZ is projected[10], then an increase in ENSO variability[8] in the coming decades appears to be a potential outcome.

Methods

Models and data. Models were selected according to data availability in the PlioMIP1 and PlioMIP2 databases. See Supplementary Table S1 for a list of the models included in our

313 analysis. A total of 9 PlioMIP1 and 16 PlioMIP2 models were analysed. PlioMIP1 and
314 PlioMIP2 boundary conditions are specified in Supplementary Table S2 and describes in
315 more detail in the Supplementary Text S1. The last 100 years of each model's simulation
316 is used.
317 **Statistical significance of the changes.** This is measured through model agreement on the
318 sign of the change. This method is based on a binomial distribution of equal probability
319 (i.e. $p = q = 0.5$). Here, we consider that all models have an equal probability of simulating
320 positive and negative changes in the mPWP simulation. As such, the cumulative
321 probability distribution function of a binomial distribution of N=9 (PlioMIP1) and N=16
322 (PlioMIP2) models shows that the 95% probability level is reached when there is a model
323 agreement on the sign of the change of 7 and 11 models, respectively.
324 **ENSO amplitude.** The standard deviation of Niño3 index is used to represent ENSO
325 amplitude. The Niño3 index is calculated from SST anomaly averaged over the eastern
326 Pacific region between 5ºN-5ºS latitude and 150º-90ºW longitude.
327 **Frequency separation.** The amplitude of decadal or higher periods is evaluated through
328 the variance of the 11-year running mean Niño3 time series in each model. The amplitude
329 of the interannual period is estimated as the variance of the residual time series, i.e. original
330 Niño3 timeseries subtracted from the Niño3 decadal timeseries.
331 **Thermocline Slope.** Difference between the mean eastern Pacific thermocline depth (5ºS-
332 5ºN; 210º-270ºW) and the western Pacific thermocline depth (5ºS-5ºN; 160º-210ºW). The
333 thermocline depths are computed from the mean temperature profile in each of the boxes
334 indicated above. This is the weighted average depth, based on depths in which the
335 temperature gradients are greater than 50% of its maximum.

Equatorial Pacific Ocean stratification. Difference between the mean temperature in the top 75 meters and the temperature at 100m from 150ºE to 140ºW, as indicated in Figure 2a.

Pacific ITCZ position[43]. The ITCZ position is taken as the average latitudes over which precipitation over the Pacific Ocean is greater than 50% of the maximum zonally averaged precipitation over 120ºE-90ºW. This method may take into account double-ITCZ and double-ITCZ biases if the double-ITCZ associated precipitation is greater than 50% of the maximum.

Criteria for model selection[11]**.** Models were selected according to their ability to simulate ENSO non-linear characteristics. Selected models were required to have DJF Niño3 precipitation greater than 5 mm per day and precipitation skewness greater than 1 in the pre-industrial control run. Out of 14 PlioMIP2 models, five models met these criteria (Supplementary Figure S6). The skewness criterion filters out models that systematically simulate overly wet and dry conditions in the eastern equatorial Pacific. These biases tend to reduce rainfall skewness in the models as they simulate SSTs well below or above the convective threshold of 26-28ºC[55], affecting Niño3 precipitation variability.

Atmospheric Subtropical High systems. Quantifying the intensity of the subtropical highs is not a simple task when dealing with different climate backgrounds (+ 2–3K) as the global pressure weakens in a warmer atmosphere. To overcome this pressure issue, we compute the streamfunction at 850 hPa to identify the position and intensity of the Subtropical High systems.

South Pacific Meridional Mode amplitude. Computed as the amplitude (standard deviation) of mean SST anomalies from 15ºS to 25ºS and from 250ºW to 260ºW.

Southern Hemisphere Booster amplitude. Computed as the amplitude (standard deviation) of meridional wind anomalies from 10ºS to 30ºS and from 140ºW to 170ºW.

CAM4 experiments. We undertook four experiments, with multiple ensemble members, using the NCAR Community Atmospheric Model version 4 (CAM4): 1) mean mid-Pliocene SST and sea-ice forcing from PlioMIP1. PlioMIP1 SST and sea-ice were time and ensemble averaged to force the CAM4 model; 2) mean pre-industrial SST and sea-ice as simulated by PlioMIP1 models for comparison; experiments 3 and 4 consisted in repeating experiments 1 and 2 but with PlioMIP2 SST and sea-ice. For each experiment 5 ensemble members were integrated with slightly different initial conditions: each ensemble member was initialised from a different day of the year. The CO_2 forcing was kept as pre-industrial at 280 ppm and no changes over continental areas were made in all experiments. Each experiment was run for 31 years. The first year of each simulation was discarded due to the atmospheric spin-up. To check if non-linearities in ENSO affected the mean SST change we compared the multi-model mean mPWP warming during all years and during non-ENSO years only. Differences in the tropical Pacific were approximately two orders of magnitude (<0.05 K) lower than the mean tropical Pacific warming (~2 K).

Acknowledgments

This work was supported by the São Paulo Research Foundation (FAPESP-Brazil grant no. 2016/23670-0 and no. 2019/0882-1) and the Australian Research Council (ARC FT160100495) including the ARC Centre of Excellence for Climate Extremes (CE110001028) and the NCI National Facility, Canberra. PlioMIP2 experiments were supported by FP7 Ideas Programme: European Research Council, Past Earth Network,

CEMAC – University of Leeds, JSPS, Earth Simulator at JAMSTEC, Helmholtz Climate Initiative REKLIM, Alfred Wegener Institute's research programme Marine, Coastal and Polar Systems, Swedish Research Council, Swedish National Infrastructure for Computing, Canadian Innovation Foundation, UNINETT Sigma2 – the National Infrastructure for High Performance Computing and Data Storage in Norway, Très Grand Centre de calcul du CEA – GENCI, National Science Foundation (NSF – USA), SURFsara Dutch National Computing and Netherlands Organisation for Scientific Research, Exact Sciences.

Author contributions

GMP, AST, ASG and AS designed the study. GMP, AST, ASG, AS and IW contributed to the interpretation of the data and discussions. GMP conducted the analysis, prepared the figures and wrote the original manuscript. ASG produced the schematic in Figure 6. GMP and AST performed the CAM4 experiments. The remaining authors performed the PlioMIP2 simulations and commented on the manuscript.

Competing Interests

The authors declare no competing interests.

Code availability

Computer codes are available upon request to Gabriel M. Pontes (gabrielpontes@usp.br).

Data availability

PlioMIP2 data (with exception of IPSLCM6A and GISS2.1G) is available upon request to Alan M. Haywood (a.m.haywood@leeds.ac.uk). PlioMIP2 data from CESM2, EC-Earth3.3, NorESM1-F, IPSLCM6A and GISS2.1G can be obtained directly through the Earth System Grid Federation repository (ESGF; https://esgf-node.llnl.gov/search/cmip6/).

References

1. McPhaden, M. J., Zebiak, S. E. & Glantz, M. H. ENSO as an integrating concept in earth science. *Science* **314**, 1740–1745 (2006).
2. Santoso, A. *et al.* Dynamics and predictability of El Niño-Southern oscillation: An Australian perspective on progress and challenges. *Bull. Am. Meteorol. Soc.* **100**, 403–420 (2019).
3. van Oldenborgh, G. J., Philip, S. Y. & Collins, M. El Niño in a changing climate: a multi-model study. *Ocean Sci.* **1**, 81–95 (2005).
4. Collins, M. *et al.* The impact of global warming on the tropical Pacific Ocean and El Nĩo. *Nat. Geosci.* **3**, 391–397 (2010).
5. Kim, S. T. & Yu, J. The two types of ENSO in CMIP5 models. *Geophys. Res. Lett.* **39**, (2012).
6. Stevenson, S. L. Significant changes to ENSO strength and impacts in the twenty-first century: Results from CMIP5. *Geophys. Res. Lett.* **39**, (2012).
7. Taschetto, A. S. *et al.* Cold Tongue and Warm Pool ENSO Events in CMIP5: Mean State and Future Projections. *J. Clim.* **27**, 2861–2885 (2014).
8. Cai, W. *et al.* Increased variability of eastern Pacific El Niño under greenhouse warming. *Nature* **564**, 201–206 (2018).
9. Santoso, A. *et al.* Late-twentieth-century emergence of the El Niño propagation asymmetry and future projections. *Nature* **504**, 126–130 (2013).
10. Cai, W. *et al.* ENSO and greenhouse warming. *Nature Climate Change* **5**, 849–859 (2015).
11. Cai, W. *et al.* Increasing frequency of extreme El Niño events due to greenhouse warming. *Nat. Clim. Chang.* **4**, 111–116 (2014).
12. Mamalakis, A. *et al.* Zonally contrasting shifts of the tropical rain belt in response to climate change. *Nat. Clim. Chang.* 1–9 (2021). doi:10.1038/s41558-020-00963-x
13. Emile-Geay, J. *et al.* Links between tropical Pacific seasonal, interannual and orbital variability during the Holocene. *Nature Geoscience* **9**, 168–173 (2016).
14. Grothe, P. R. *et al.* Enhanced El Niño-Southern Oscillation variability in recent decades. *Geophys. Res. Lett.* (2019). doi:10.1029/2019gl083906
15. Tierney, J. E. *et al.* Past climates inform our future. *Science (80-.).* **370**, (2020).
16. Rickaby, R. E. M. & Halloran, P. Cool La Niña during the warmth of the Pliocene? *Science (80-.).* **307**, 1948–1952 (2005).
17. Wara, M. W., Ravelo, A. C. & Delaney, M. L. Permanent El Niño-like Conditions

during the Pliocene Warm Period. *Source Sci. New Ser.* **309**, 758–761 (2005).
18. Brierley, C. M. *et al.* Greatly Expanded Tropical Warm Pool and Waekened Hadley Circulation in the Early Pliocene. *Science (80-.).* **323**, 1714–1718 (2009).
19. Watanabe, T. *et al.* Permanent El Niño during the Pliocene warm period not supported by coral evidence. *Nature* **471**, 209–211 (2011).
20. Burke, K. D. *et al.* Pliocene and Eocene provide best analogs for near-future climates. *Proc. Natl. Acad. Sci. U. S. A.* **115**, 13288–13293 (2018).
21. Yan, Q., Wang, H., Johannessen, O. M. & Zhang, Z. Greenland ice sheet contribution to future global sea level rise based on CMIP5 models. *Adv. Atmos. Sci.* **31**, 8–16 (2014).
22. Haywood, A. M., Dowsett, H. J. & Dolan, A. M. Intregation geological archives and climate models for the mid-Pliocene warm period. *Nat. Commun.* **6**, 1–14 (2016).
23. Seki, O. *et al.* Alkenone and boron-based Pliocene pCO2 records. *Earth Planet. Sci. Lett.* **292**, 201–211 (2010).
24. Hill, D. J. *et al.* Evaluating the dominant components of warming in Pliocene climate simulations. *Clim. Past* **10**, 79–90 (2014).
25. Haywood, A. M. *et al.* Pliocene Model Intercomparison Project (PlioMIP): experimental design and boundary conditions (Experiment 2). *Geosci. Model Dev.* **4**, 571–577 (2011).
26. Haywood, A. M. *et al.* The Pliocene Model Intercomparison Project (PlioMIP) Phase 2 : scientific objectives and experimental design. *Clim. Past* **12**, 663–675 (2016).
27. Pontes, G. M., Wainer, I., Prado, L. & Brierley, C. Reduced Atlantic variability in the mid-Pliocene. *Clim. Change* **160**, 445–461 (2020).
28. Jin, F. F., Kim, S. T. & Bejarano, L. A coupled-stability index for ENSO. *Geophys. Res. Lett.* **33**, L23708 (2006).
29. Oldeman, A. M. *et al.* Reduced El-Niño variability in the mid-Pliocene according to the PlioMIP2 ensemble. *in prep.* (2021).
30. Xie, S.-P. *et al.* Global Warming Pattern Formation: Sea Surface Temperature and Rainfall. *J. Clim.* **23**, 966–986 (2010).
31. Wang, B. *et al.* Historical change of El Niño properties sheds light on future changes of extreme El Niño. *Proc. Natl. Acad. Sci. U. S. A.* **116**, 22512–22517 (2019).
32. Manucharyan, G. E. & Fedorov, A. V. Robust ENSO across a wide range of climates. *J. Clim.* **27**, 5836–5850 (2014).
33. Hong, L.-C., LinHo & Jin, F.-F. A Southern Hemisphere booster of super El Niño. *Geophys. Res. Lett.* **41**, 2142–2149 (2014).
34. Larson, S. & Kirtman, B. The Pacific Meridional Mode as a trigger for ENSO in a high-resolution coupled model. *Geophys. Res. Lett.* **40**, 3189–3194 (2013).
35. Haywood, A. M. *et al.* The Pliocene Model Intercomparison Project Phase 2: large-scale climate features and climate sensitivity. *Clim. Past* **16**, 2095–2123 (2020).
36. Timmermann, A. *et al.* El Niño–Southern Oscillation complexity. *Nature* **559**, 535–545 (2018).
37. Chen, D. *et al.* Strong influence of westerly wind bursts on El Niño diversity.

Nature Geoscience **8**, 339–345 (2015).
38. Haywood, A. M. *et al.* Large-scale features of Pliocene climate: Results from the Pliocene Model Intercomparison Project. *Clim. Past* **9**, 191–209 (2013).
39. Schneider, T., Bischoff, T. & Haug, G. H. Migrations and dynamics of the intertropical convergence zone. *Nature* **513**, 45–53 (2014).
40. Donohoe, A., Marshall, J., Ferreira, D. & Mcgee, D. The Relationship between ITCZ Location and Cross-Equatorial Atmospheric Heat Transport: From the Seasonal Cycle to the Last Glacial Maximum. *J. Clim.* **June**, 3597–3618 (2013).
41. Mcgee, D. *et al.* Hemispherically asymmetric trade wind changes as signatures of past ITCZ shifts. *Quat. Sci. Rev.* **180**, 214–228 (2018).
42. Yun, K. S., Timmermann, A. & Stuecker, M. Synchronized spatial shifts of Hadley and Walker circulations. *Earth Syst. Dyn.* **12**, 121–132 (2021).
43. Pontes, G. M. *et al.* Drier tropical and subtropical Southern Hemisphere in the mid-Pliocene Warm Period. *Sci. Rep.* **10**, 13458 (2020).
44. Chiang, J. C. H. & Friedman, A. R. Extratropical Cooling, Interhemispheric Thermal Gradients, and Tropical Climate Change. *Annu. Rev. Earth Planet. Sci.* **40**, 383–412 (2012).
45. Cai, W. *et al.* Pantropical climate interactions. *Science* **363**, eaav4236 (2019).
46. Dommenget, D. & Yu, Y. The effects of remote SST forcings on ENSO dynamics, variability and diversity. *Clim. Dyn.* **49**, 2605–2624 (2017).
47. Dommenget, D., Semenov, V. & Latif, M. Impacts of the tropical Indian and Atlantic Oceans on ENSO. *Geophys. Res. Lett.* **33**, 2006GL025871 (2006).
48. Ham, Y. G., Kug, J. S., Park, J. Y. & Jin, F. F. Sea surface temperature in the north tropical Atlantic as a trigger for El Niño/Southern Oscillation events. *Nat. Geosci.* **6**, 112–116 (2013).
49. Fedorov, A. V. *et al.* Patterns and mechanisms of early Pliocene warmth. *Nature* **496**, 43–49 (2013).
50. Koenig, S. J. *et al.* Ice sheet model dependency of the simulated Greenland Ice Sheet in the mid-Pliocene. *Clim. Past* **11**, 369–381 (2015).
51. Et al., T. N. Obliquity-paced Pliocene West Antarctic ice sheet oscillations. *Nature* **458**, 322–329 (2009).
52. Fischer, H. *et al.* Palaeoclimate constraints on the impact of 2 °c anthropogenic warming and beyond. *Nature Geoscience* **11**, 474–485 (2018).
53. Zhu, J., Poulsen, C. J. & Otto-Bliesner, B. L. High climate sensitivity in CMIP6 model not supported by paleoclimate. *Nature Climate Change* **10**, 378–379 (2020).
54. Tian, B. & Dong, X. The Double-ITCZ Bias in CMIP3, CMIP5 and CMIP6 Models Based on Annual Mean Precipitation. *Geophys. Res. Lett.* e2020GL087232 (2020). doi:10.1029/2020GL087232
55. Johnson, N. C. & Xie, S. P. Changes in the sea surface temperature threshold for tropical convection. *Nat. Geosci.* **3**, 842–845 (2010).

Figures

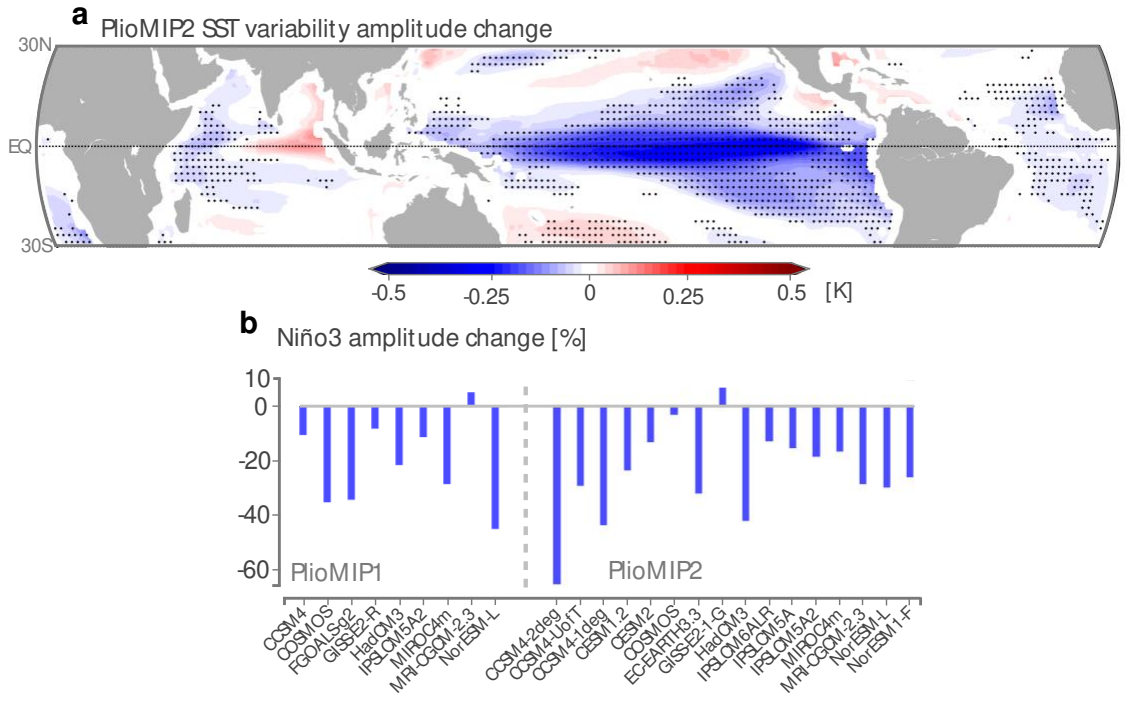

Figure 1 – Simulated Mid-Pliocene tropical variability changes. a) multi-model mean change in the amplitude (variance) of SST variability in the PlioMIP2 models (see Supplementary Figure S1 for PlioMIP1 models). Stippling indicates locations where there is a significant model agreement (at least 70%) in the sign of the change. b) change in the amplitude (standard deviation) of the Niño3 (5ºS-5ºN; 210º-270ºE) time series in each PlioMIP model.

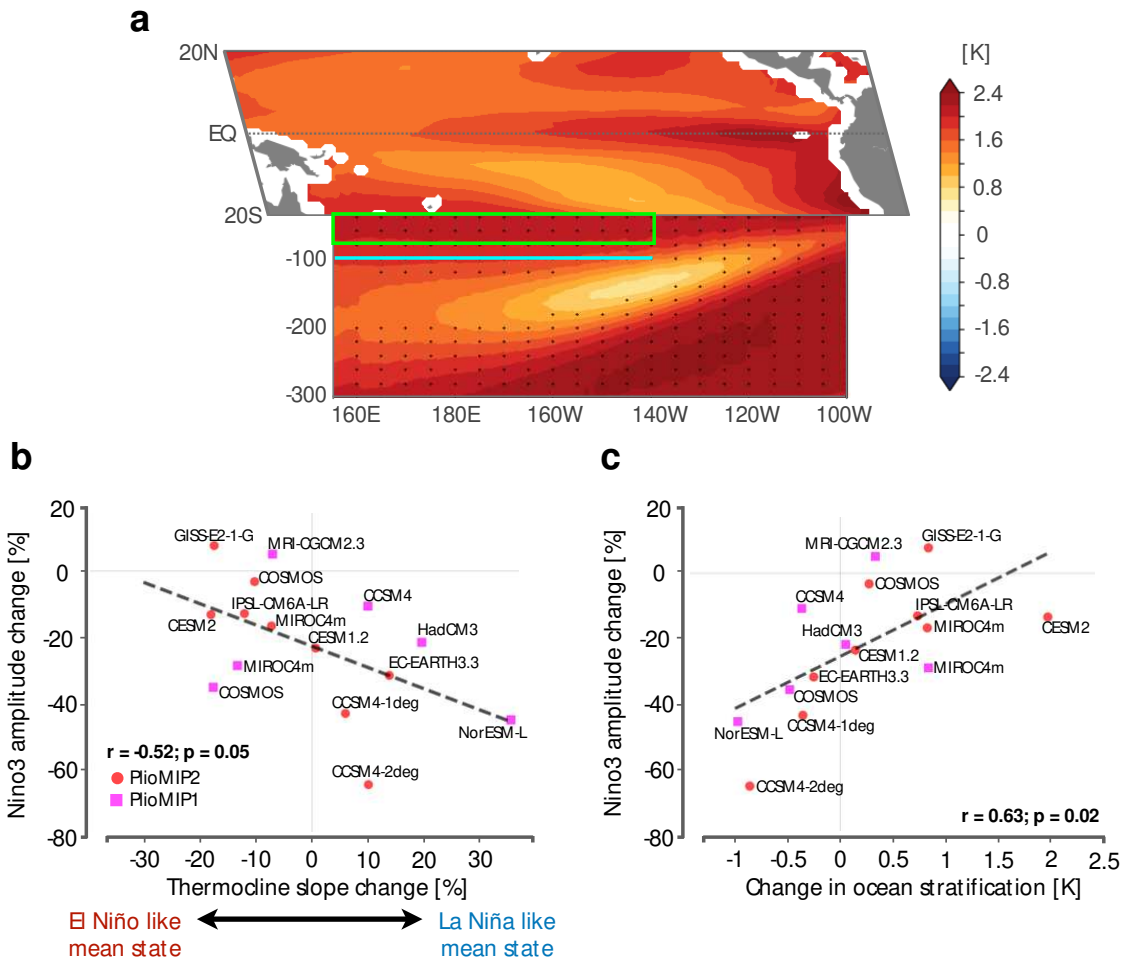

Figure 2 – Equatorial Pacific Ocean changes. a) PlioMIP2 multi-model mean change in surface tropical and sub-surface equatorial Pacific temperatures. The vertical profile is averaged between 5ºS and 5ºN. Stippling indicates significant change at the 95% level (in the SST panel the entire basin-wide warming is significant at the 95% level). See Supplementary Figures S3 and S4 for individual PlioMIP2 models and Supplementary Figures S5 and S6 for PlioMIP1 models. b) inter-model relationship between the change in the thermocline slope between the eastern and western Pacific (see Methods) and the change in the Niño3 amplitude. c) inter-model relationship between the change in ocean stratification and in the Niño3 amplitude. Ocean stratification was measured as the difference between the average temperature in the top 75m (green box, panel a) and at 100m (blue line), from 150ºE to 140ºW.

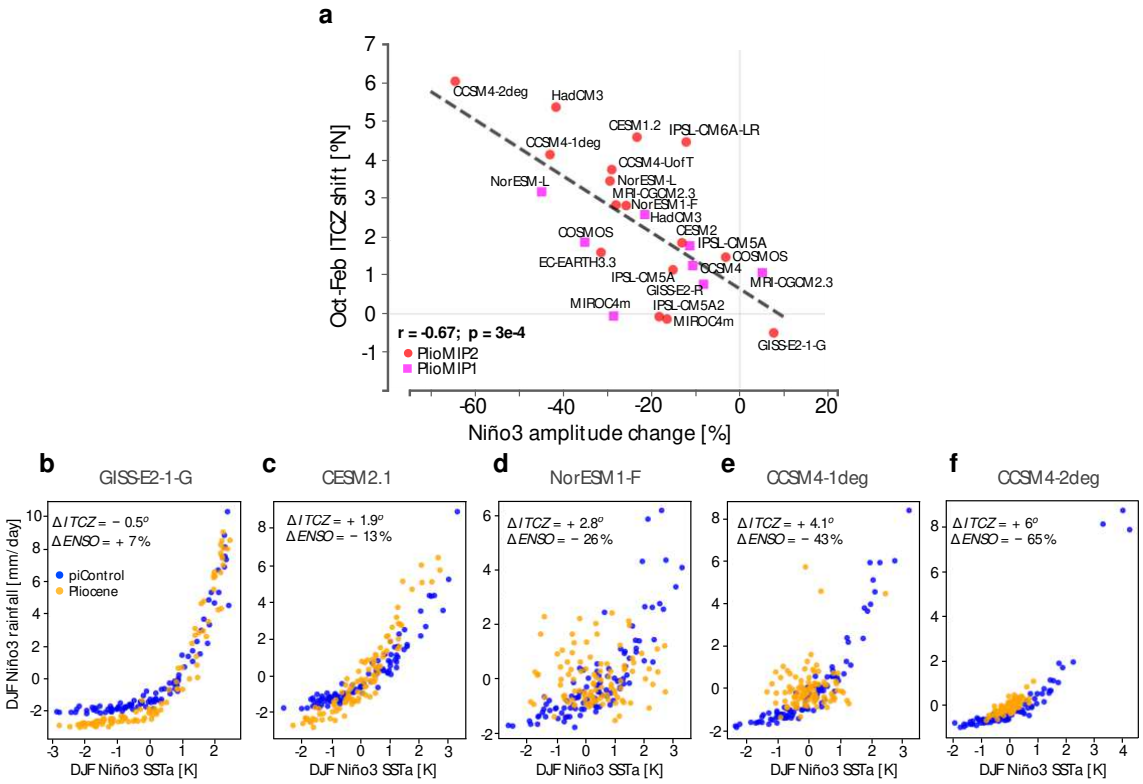

559

560 Figure 3 – ENSO-ITCZ inter-model relationship. a) PlioMIP2 inter-model relationship
561 between the change in the Niño3 amplitude and mean ITCZ shift from October to February.
562 b) to f) model relationship between DJF Niño3 SST anomalies and DJF Niño3 rainfall
563 anomalies for pre-industrial (blue) and mid-Pliocene simulations (yellow). Models were
564 selected according to their ability to simulate non-linear ENSO characteristics (See
565 Methods). PlioMIP1 precipitation data for the last 100 years was not available so these
566 models could not be included in this analysis (see Methods).
567

568

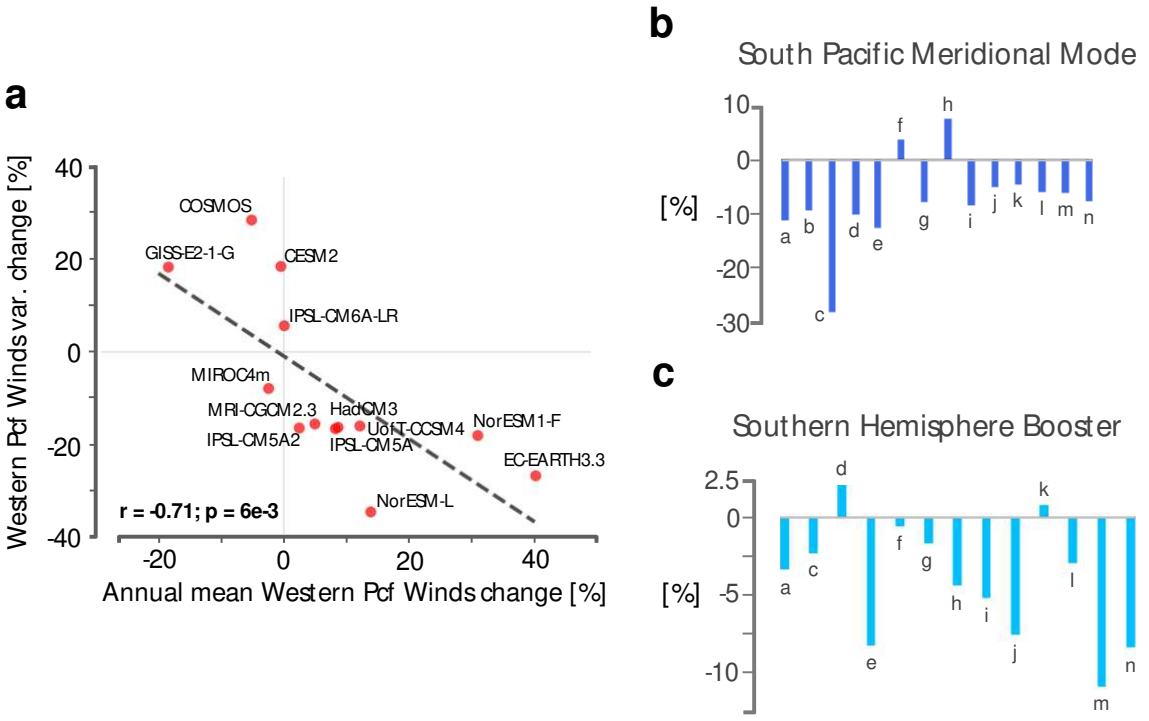

Figure 4 – Changes to potential ENSO triggers. a) inter-model relationship between the change in the intensity of the western Pacific trade winds (from 160ºE to 150ºW and from 10ºS to 10ºN) and the amplitude (standard deviation) of its monthly variability. To ideally examine changes in the western wind bursts we would daily output, however high frequency output was not available for the PlioMIP models. b) Change in the amplitude (standard deviation) of the South Pacific Meridional mode time series, defined as the mean SST anomaly between 15ºS-25ºS and 250ºW-260ºW. c) Change in the amplitude (standard deviation) of the meridional wind variability over the Southern Hemisphere Booster region (from 10ºS to 30ºS and from 140ºW to 170ºW). PlioMIP2 models in panels 'b' and 'c': a – CCSM4-UofT; b – CCSM4-2deg; c – CESM2; d – COSMOS; e – EC-EARTH3.3; f – GISS-E2-1-G; g – HadCM3; h – IPSL-CM6A-LR; i – IPSL-CM5A; j – IPSL-CM5A2; k – MIROC4m; l – MRI-CGCM2.3; m – NorESM-L; n – NorESM1-F.

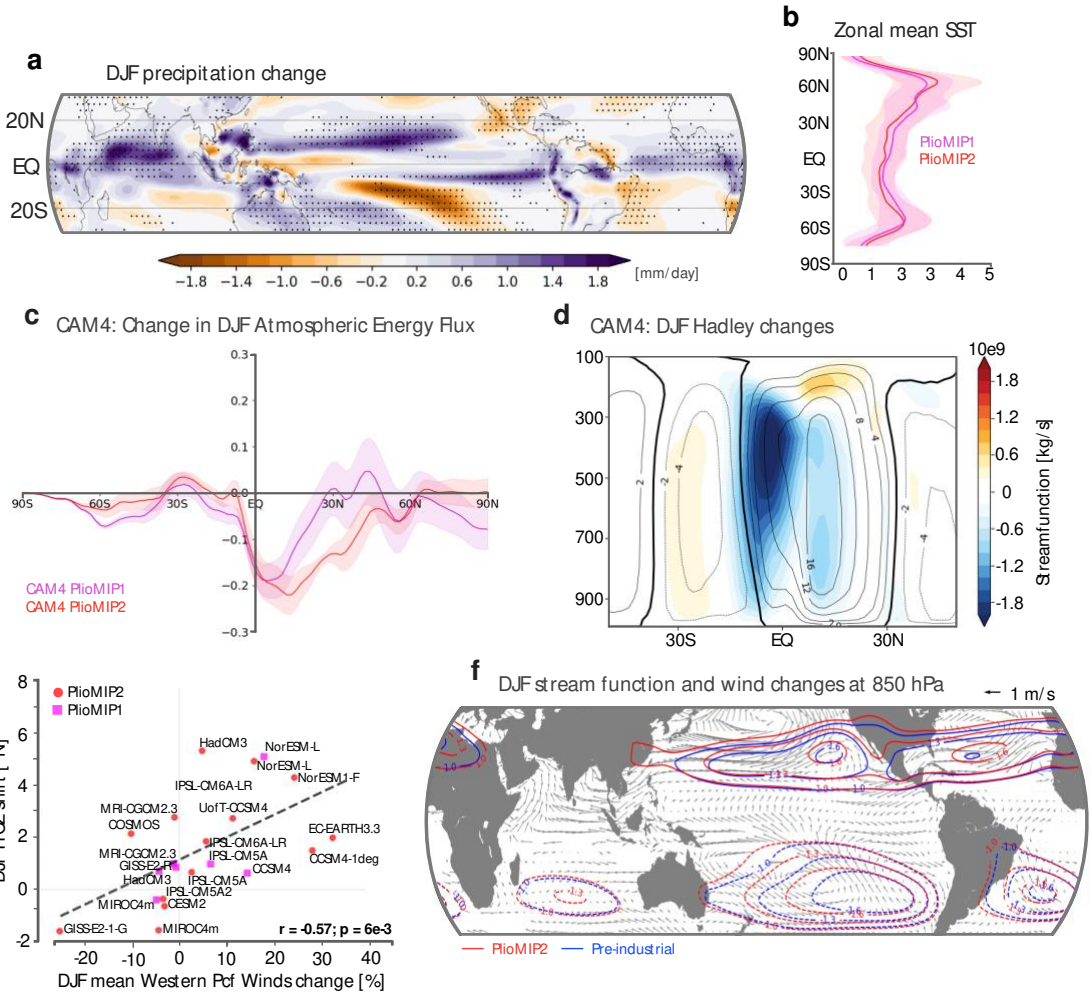

584

585 Figure 5 – Energetics constraints for the ITCZ position. a) DJF precipitation change in the
586 PlioMIP2 models (mPWP minus pre-industrial). Stippling indicates where the change is
587 significant at the 95% level. b) multi-model mean change zonally averaged SST for the
588 PlioMIP1 (magenta) and PLioMIP2 (red). Banding indicates standard deviation range. c)
589 Changes in DJF atmospheric energy flux, computed as the residual between the total top-
590 of-the-atmosphere and surface energy fluxes, in the CAM4 experiments forced with
591 PlioMIP1 and 2 climatological SST and sea-ice (see Methods). Banding indicates standard
592 deviation range of a 5-member ensemble. d) Changes in the meridional streamfunction in
593 the CAM4 experiment forced with PlioMIP2 SST and sea-ice (see Methods). y-axis:
594 Pressure [mb]. Contours indicate pre-industrial streamfunction (zero contour in bold).
595 Colours indicate change (mPWP minus pre-industrial) e) Inter-model relationship between
596 changes in the intensity of the zonal western Pacific trades and ITCZ shift during austral
597 summer. f) Changes in global low-level (850 hPa) winds and stream function in the
598 PlioMIP2 models. Wind changes are only plotted where there is a significant change at the
599 95% level.
600

601

602

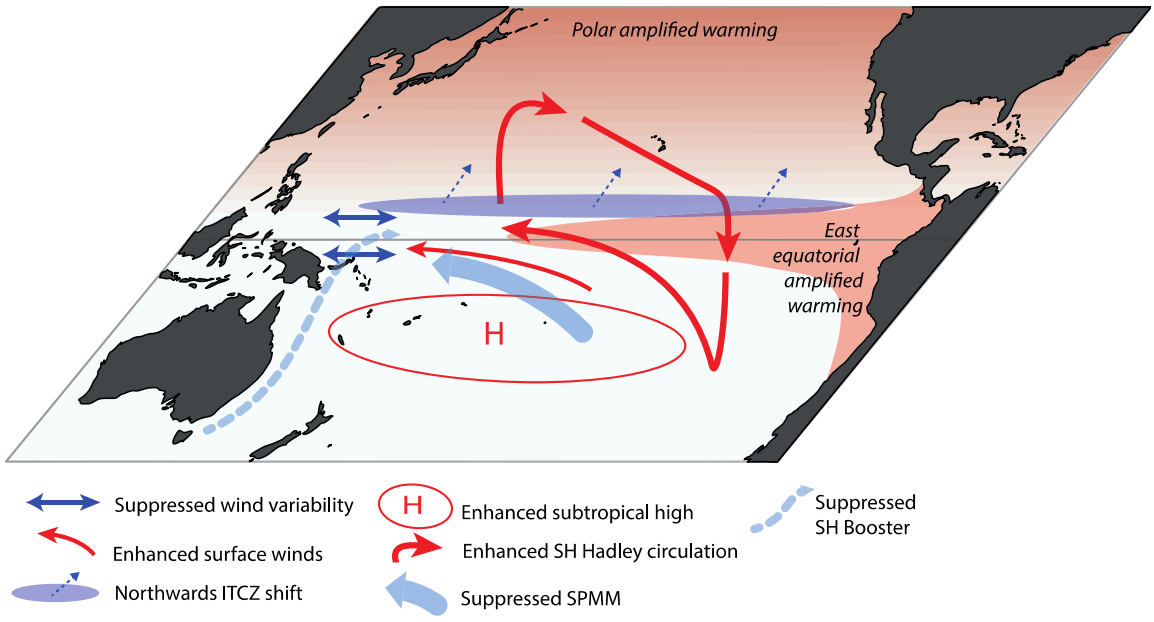

603

604 Figure 6 – Schematic of the drivers of suppressed ENSO activity in the mPWP. A
605 northward ITCZ shift reduces the probability of occurrence of deep convection in the
606 central-eastern Pacific. Energetic constrains for the ITCZ position indicates that higher
607 rates of warming in Northern Hemisphere drive a northward ITCZ shift and intensified
608 enhanced Southern Hemisphere Hadley circulation. These changes are also associated with
609 enhanced subtropical high and intensified western Pacific trades. Enhanced trade winds
610 suppress wind variability in the western Pacific, which are important for El Niño initiation.
611 An intensified subtropical high is thought to impede zonal pressure anomalies across the
612 tropical South Pacific and, thus, suppress the activity of the South Pacific Meridional Mode
613 (SPMM) and Southern Hemisphere Booster that are important for the development of
614 strong El Niño events.

Figures

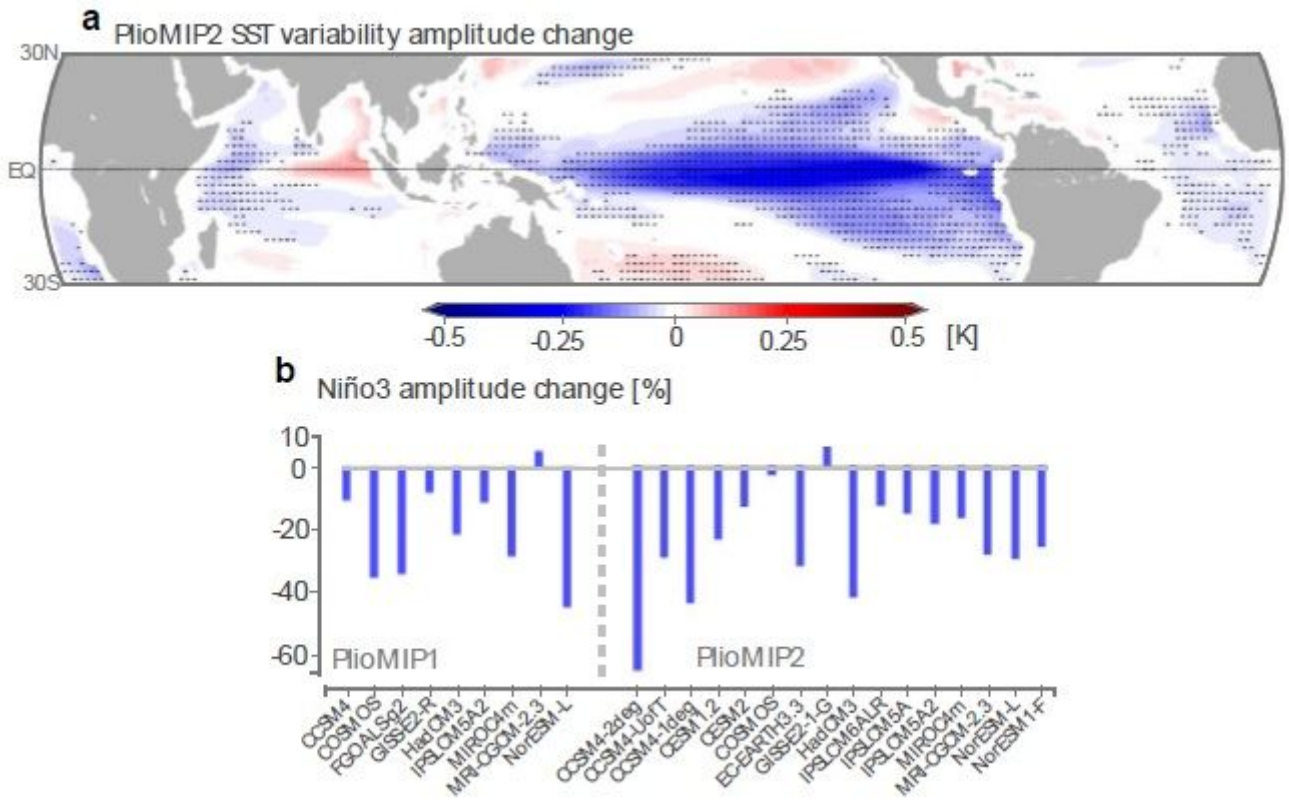

Figure 1

Simulated Mid-Pliocene tropical variability changes. a) multi-model mean change in the amplitude (variance) of SST variability in the PlioMIP2 models (see Supplementary Figure S1 for PlioMIP1 models). Stippling indicates locations where there is a significant model agreement (at least 70%) in the sign of the change. b) change in the amplitude (standard deviation) of the Niño3 (5ºS-5ºN; 210º-270ºE) time series in each PlioMIP model. Note: The designations employed and the presentation of the material on this map do not imply the expression of any opinion whatsoever on the part of Research Square concerning the legal status of any country, territory, city or area or of its authorities, or concerning the delimitation of its frontiers or boundaries. This map has been provided by the authors.

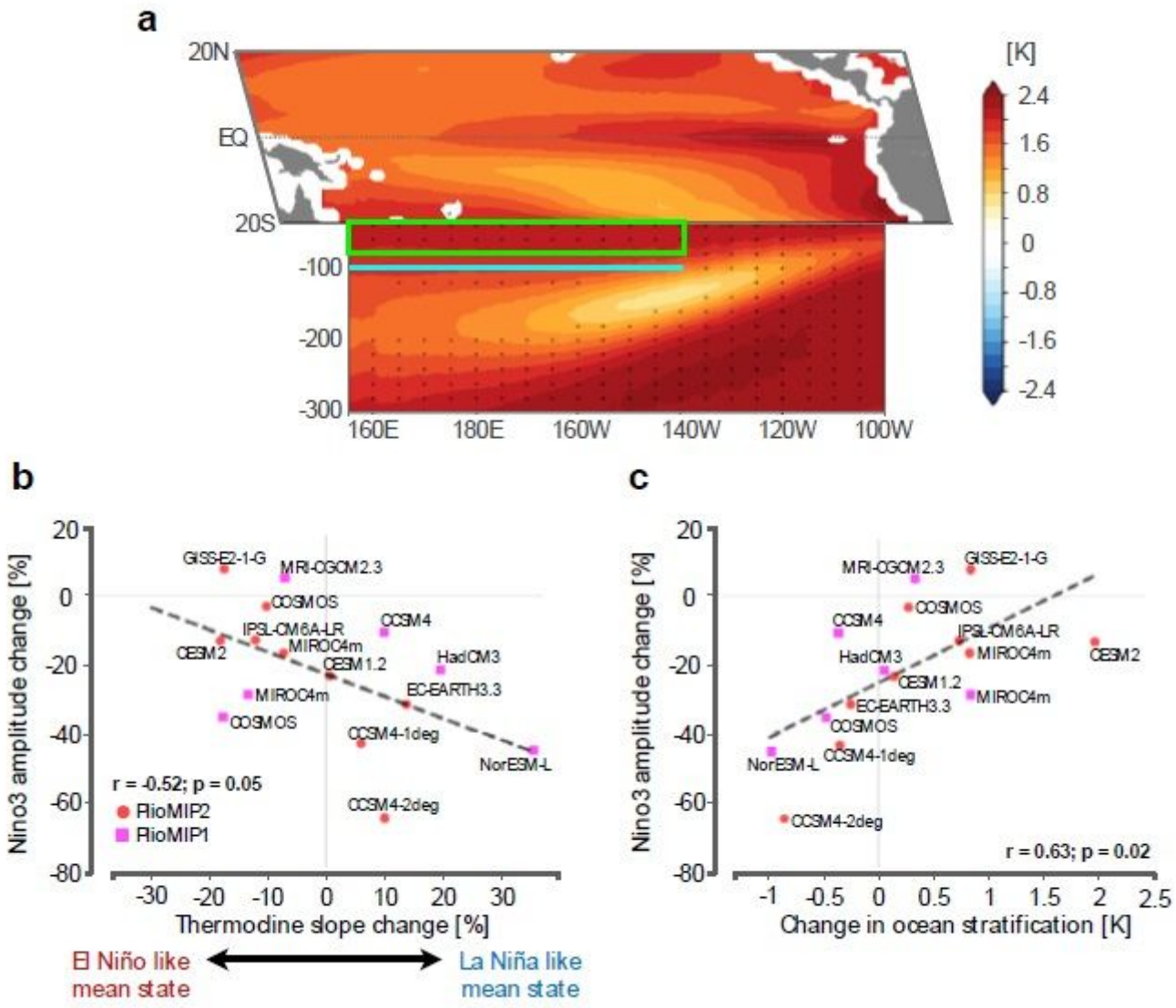

Figure 2

Equatorial Pacific Ocean changes. a) PlioMIP2 multi-model mean change in surface tropical and sub-surface equatorial Pacific temperatures. The vertical profile is averaged between 5ºS and 5ºN. Stippling indicates significant change at the 95% level (in the SST panel the entire basin-wide warming is significant at the 95% level). See Supplementary Figures S3 and S4 for individual PlioMIP2 models and Supplementary Figures S5 and S6 for PlioMIP1 models. b) inter-model relationship between the change in the thermocline slope between the eastern and western Pacific (see Methods) and the change in the Niño3 amplitude. c) inter-model relationship between the change in ocean stratification and in the Niño3 amplitude. Ocean stratification was measured as the difference between the average temperature in the top 75m (green box, panel a) and at 100m (blue line), from 150ºE to 140ºW.

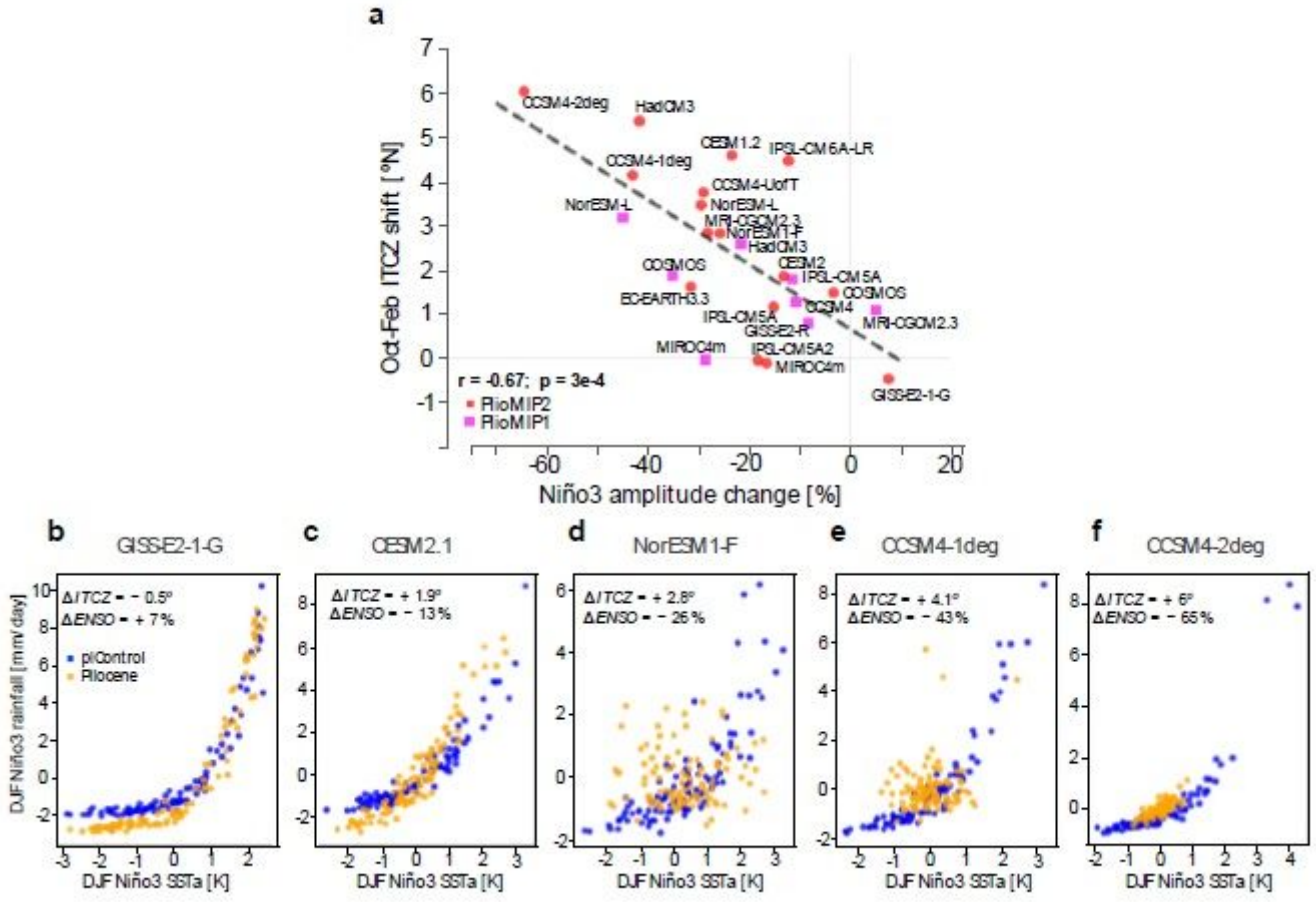

Figure 3

ENSO-ITCZ inter-model relationship. a) PlioMIP2 inter-model relationship between the change in the Niño3 amplitude and mean ITCZ shift from October to February. b) to f) model relationship between DJF Niño3 SST anomalies and DJF Niño3 rainfall anomalies for pre-industrial (blue) and mid-Pliocene simulations (yellow). Models were selected according to their ability to simulate non-linear ENSO characteristics (See Methods). PlioMIP1 precipitation data for the last 100 years was not available so these models could not be included in this analysis (see Methods).

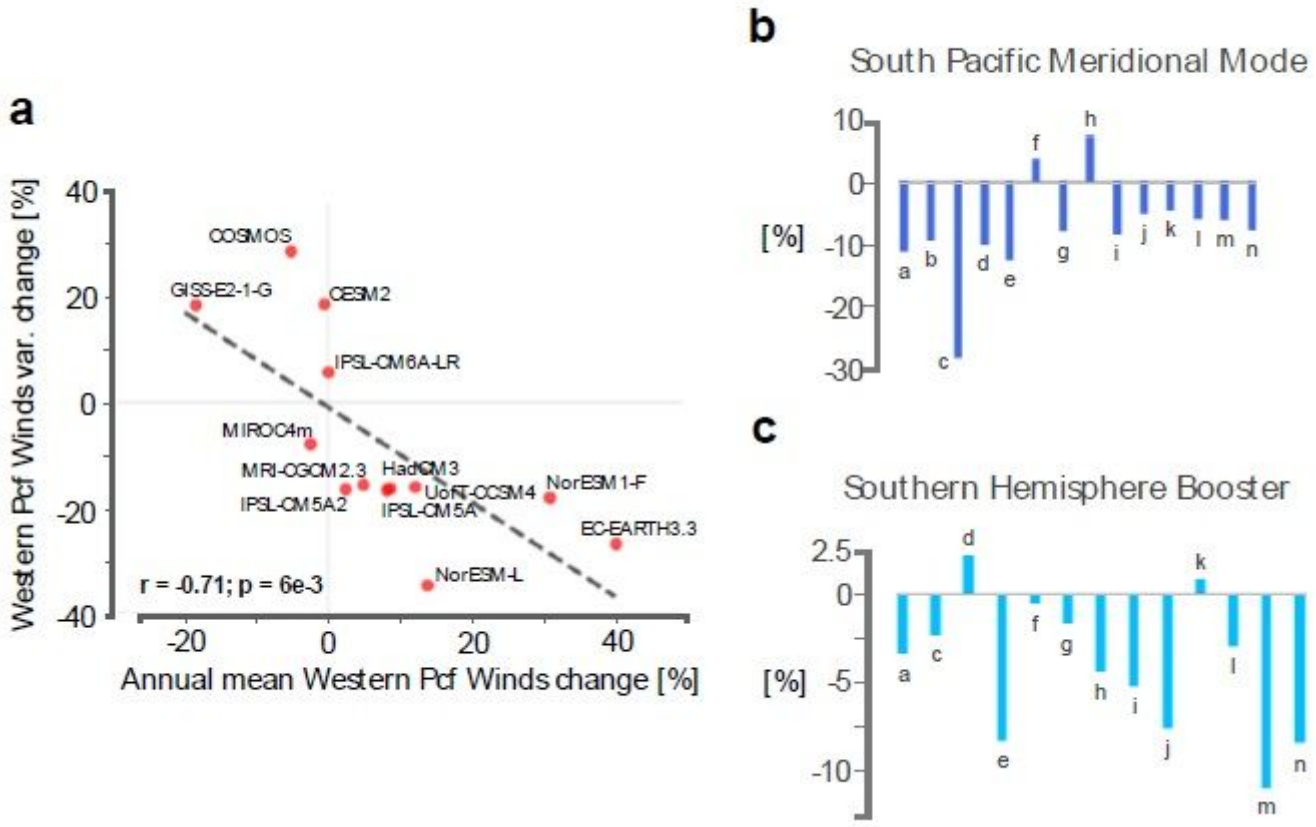

Figure 4

Changes to potential ENSO triggers. a) inter-model relationship between the change in the intensity of the western Pacific trade winds (from 160ºE to 150ºW and from 10ºS to 10ºN) and the amplitude (standard deviation) of its monthly variability. To ideally examine changes in the western wind bursts we would daily output, however high frequency output was not available for the PlioMIP models. b) Change in the amplitude (standard deviation) of the South Pacific Meridional mode time series, defined as the mean SST anomaly between 15ºS-25ºS and 250ºW-260ºW. c) Change in the amplitude (standard deviation) of the meridional wind variability over the Southern Hemisphere Booster region (from 10ºS to 30ºS and from 140ºW to 170ºW). PlioMIP2 models in panels 'b' and 'c': a – CCSM4-UofT; b – CCSM4-2deg; c – CESM2; d – COSMOS; e – EC-EARTH3.3; f – GISS-E2-1-G; g – HadCM3; h – IPSL-CM6A-LR; i – IPSL-CM5A; j – IPSL-CM5A2; k – MIROC4m; l – MRI-CGCM2.3; m – NorESM-L; n – NorESM1-F.

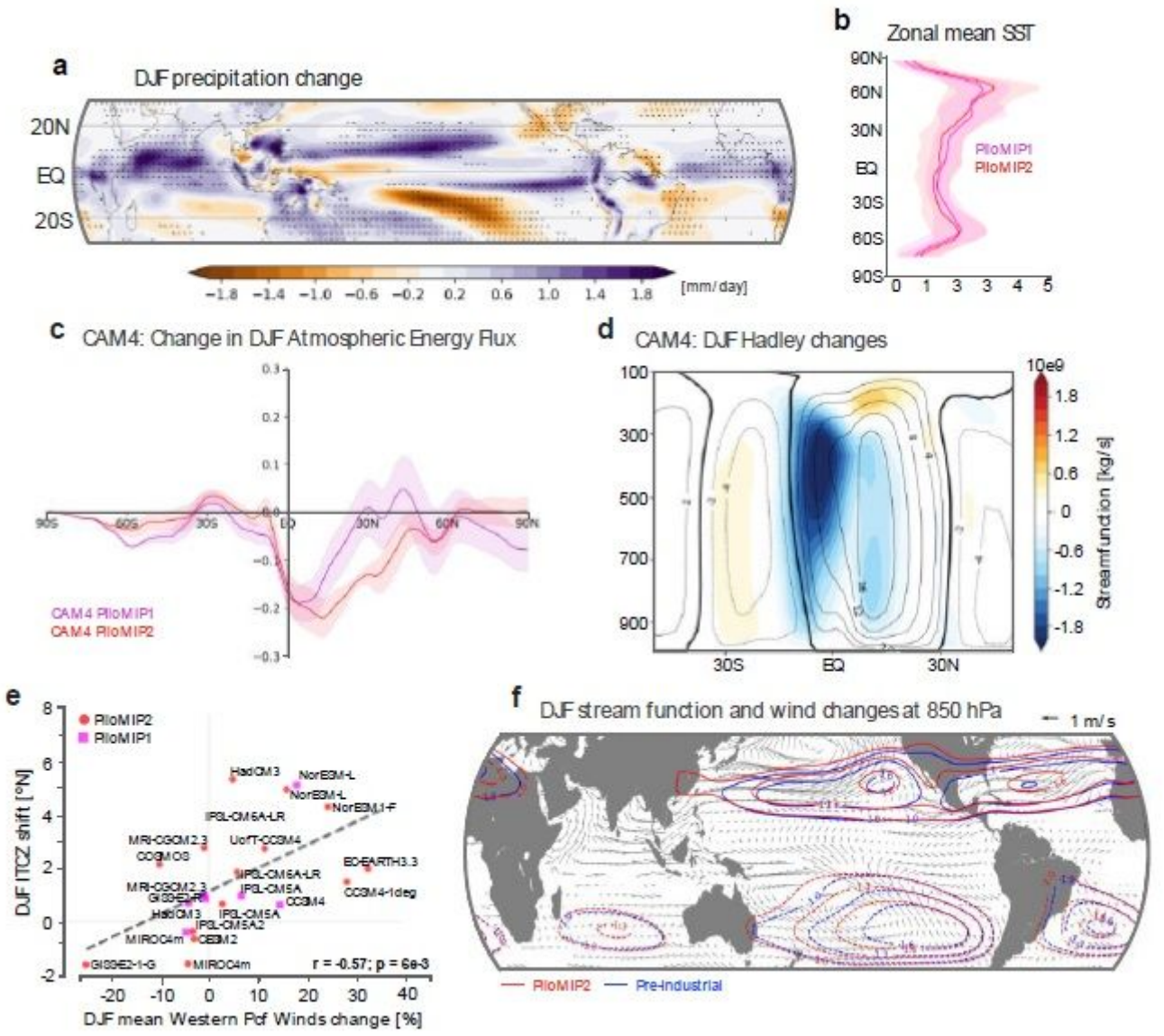

Figure 5

Energetics constraints for the ITCZ position. a) DJF precipitation change in the PlioMIP2 models (mPWP minus pre-industrial). Stippling indicates where the change is significant at the 95% level. b) multi-model mean change zonally averaged SST for the PlioMIP1 (magenta) and PLioMIP2 (red). Banding indicates standard deviation range. c) Changes in DJF atmospheric energy flux, computed as the residual between the total top-of-the-atmosphere and surface energy fluxes, in the CAM4 experiments forced with PlioMIP1 and 2 climatological SST and sea-ice (see Methods). Banding indicates standard deviation range of a 5-member ensemble. d) Changes in the meridional streamfunction in the CAM4 experiment forced with PlioMIP2 SST and sea-ice (see Methods). y-axis: Pressure [mb]. Contours indicate pre-industrial streamfunction (zero contour in bold). Colours indicate change (mPWP minus pre-industrial) e) Inter-model relationship between changes in the intensity of the zonal western Pacific trades and ITCZ shift during austral summer. f) Changes in global low-level (850 hPa) winds and stream function in the PlioMIP2 models. Wind changes are only plotted where there is a significant change at the 95% level.

Note: The designations employed and the presentation of the material on this map do not imply the expression of any opinion whatsoever on the part of Research Square concerning the legal status of any country, territory, city or area or of its authorities, or concerning the delimitation of its frontiers or boundaries. This map has been provided by the authors.

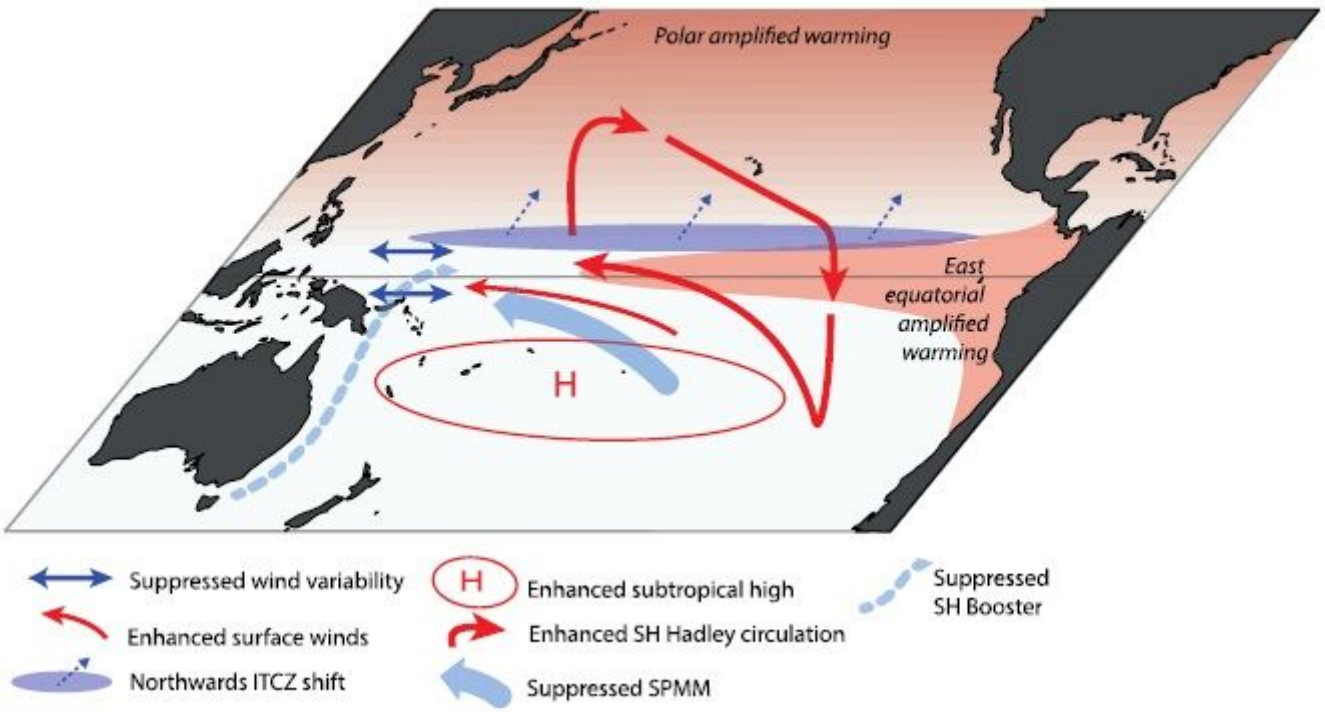

Figure 6

Schematic of the drivers of suppressed ENSO activity in the mPWP. A northward ITCZ shift reduces the probability of occurrence of deep convection in the central-eastern Pacific. Energetic constrains for the ITCZ position indicates that higher rates of warming in Northern Hemisphere drive a northward ITCZ shift and intensified enhanced Southern Hemisphere Hadley circulation. These changes are also associated with enhanced subtropical high and intensified western Pacific trades. Enhanced trade windssuppress wind variability in the western Pacific, which are important for El Niño initiation. An intensified subtropical high is thought to impede zonal pressure anomalies across the tropical South Pacific and, thus, suppress the activity of the South Pacific Meridional Mode (SPMM) and Southern Hemisphere Booster that are important for the development of strong El Niño events. Note: The designations employed and the presentation of the material on this map do not imply the expression of any opinion whatsoever on the part of Research Square concerning the legal status of any country, territory, city or area or of its authorities, or concerning the delimitation of its frontiers or boundaries. This map has been provided by the authors.

Supplementary Files

This is a list of supplementary files associated with this preprint. Click to download.

- PontesetalnewSIfinal.pdf